Solution and Solid Phase Electrochemical Behaviour of [Os(bpy)$_3$]$_3$[P$_2$W$_{18}$O$_{62}$]

Nigel Fay, Eithne Dempsey[1], and Timothy McCormac[1]*

Centre for Research in Electroanalytical Technology "CREATE"

Department of Applied Science

Institute of Technology Tallaght

Dublin 24

Ireland

Abstract

[Os(bpy)$_3$]$_3$[P$_2$W$_{18}$O$_{62}$] has been synthesised and characterised by elemental analysis, spectroscopic (UV/Vis, IR spectroscopy) and electrochemical techniques. In 0.1M Bu$_4$NPF$_6$ DMSO the complex shows a series of redox couples associated with the Os$^{3+/2+}$ and bipyridine ligands of the cationic [Os(bpy)$_3$]$^{2+}$ moiety and the tungsten-oxo framework of the associated Dawson parent heteropolyanion, [P$_2$W$_{18}$O$_{62}$]$^{6-}$. At this electrolyte concentration the Os^{3+} redox form of the complex was seen to adsorb onto the electrode surface. When the electrolyte concentration is lowered to 0.01M Bu$_4$NPF$_6$ in addition to the Os$^{3+/2+}$ redox couple, the redox process associated with the [P$_2$W$_{18}$O$_{62}$]$^{8-/7-}$ couple also exhibited properties indicating surface based processes were present. Electroactive films of the complex were formed on carbon macroelectrodes by the redox switching of the transition metal within the complex. Voltammetric investigations into the film's behaviour in a range of buffer solutions (pH 2.0, 4.5 and 7.0) were performed. The films were found to possess better stability in acidic pH and the same pH dependence for the tungsten-oxo framework of the heteropolyanions as in solution. Solid state electrochemical measurements on mechanically attached microparticles of the complex were performed, with the effect of both the nature and concentration of the aqueous electrolyte on this behaviour being investigated. Upon redox switching between the Os$^{2+/3+}$ redox states there is an associated insertion/expulsion of anions from/to the solution phase. Scanning electron micrographs of these solid state films were attained before and after redox cycling.

*to whom correspondence should be addressed

Email: tim.mccormac@it-tallaght.ie Fax: +353-1-4074200 Tel: +353-1-4042814

[1] ISE member

1. Introduction

Heteropolyanions (HPA) are an important class of inorganic cage like structures which have received widespread attention over the past few decades, primarily due to their wide range of applications in fields such as medicine [1-5], catalysis [6-12] and molecular materials [13-15], just to name a few. One of the most studied HPA families is that of the Dawson HPA, $[X_2M_{18}O_{62}]^{6-}$, where typically X is P or Si and M is W or Mo. Our group is primarily concerned with the application of this family of HPAs in the development of electrochemical sensors with the HPA acting as a possible electrocatalyst. HPAs in the past have been employed as electrocatalysts for a variety of substrates, such as, NO [16-24], H_2O_2 [25-28], NADH [29-32] and the hydrogen evolution reaction [33-36]. A crucial step in the development of any electrochemical based sensor is the immobilisation of the electrocatalyst onto the electrode surface. Various techniques have in the past been employed for the immobilisation of HPAs, such as, electrodeposition [37-43], conducting polymers [44-48] and adsorption [49-54]. Recently surface modification by HPAs through the development of self assembled monolayers has been undertaken by various groups [55-59]. In some of the latter cases [57,58] this has involved the construction of multilayer assemblies on electrode surfaces through the exploitation of the HPAs ability to attract and bond multiply-charged cations such as $M(bpy)_3^{2+}$, where M is Os^{2+}, Ru^{2+}, Fe^{2+}. Recently, in order to probe the interactions that can take place in these multilayer systems between the two components Hultgren *et al*. [60] reported the synthesis and electrochemical properties of the complex $[Ru(bpy)_3]_2[Si_2Mo_{18}O_{62}]$. They performed studies into the electrochemical solution behaviour of the complex and their conclusion was that the electrochemical behaviour of both the HPA and the $Ru(bpy)_3^{2+}$ is altered upon complexation, with the role of the electrolyte being of paramount importance. However, only preliminary work on the solid state electrochemical behaviour of this complex was undertaken. Another group [61] have synthesised and employed a bifunctional electrocatalyst based upon the reaction between $Ru(bpy)_3^{2+}$ and 12-molybdophosphate. Han *et al* [62] have reported the X-ray crystallographic study of the first tris-(2,2'-bpy) ruthenium complex with a decatungstate cluster anion. Our group is interested in synthesising and performing solid state studies on materials based on the complexation between $M(bpy)_3^{2+}$ (M is Os^{2+}, Fe^{2+}, Ru^{2+}, Ni^{2+}) and Dawson type HPAs. These possess various redox processes

that can be probed to study the materials solid state properties, such as, heterogeneous and homogeneous charge transport dynamics and ion intercalation processes. Various groups [63-69] have studied a range of redox active materials attached to electrode surfaces, with some of these exhibiting rapid ion insertion/ expulsion properties upon redox switching. However to the best of our knowledge solid state electrochemical studies based on HPAs has received little attention. This is somewhat surprising considering the properties that HPAs possess. The successful synthesis of these novel types of HPA complexes may lead to a new family of potential solid state redox active materials that may have applications in areas such as sensors, energy storage, electrochromic devices and supercapacitors [70-72]. In this paper we present the synthesis, characterisation, solution and solid state electrochemical behaviour of the $[Os(bpy)_3]_3[P_2W_{18}O_{62}]$ complex.

2. Experimental

2.1 Materials

α/β-$K_6P_2W_{18}O_{62}$.15H_2O was synthesised as described previously [73]. [Os(bpy)$_3$]Cl$_2$ was synthesised according to the literature [74]. All other chemicals were of reagent grade and used as received. HPLC grade dimethylsulphoxide (DMSO) and acetonitrile (MeCN) were dried according to conventional means prior to use. Aqueous buffer solutions were prepared according to the literature [75]. The complex was synthesised according to the published procedure [60], and then characterised by elemental analysis, spectroscopic (IR, UV/Vis) and electrochemical techniques. Elemental analysis calculated (found): [Os(bpy)$_3$]$_3$[P$_2$W$_{18}$O$_{62}$]; C 17.03 (17.04); H 1.42 (1.16); N 3.97 (3.33); P 0.98 (0.84).

2.2. Apparatus and Procedures

The reference electrode that was employed in organic solvents was a silver wire in contact with a solution of AgNO$_3$ (0.01M) and 0.1M of the same supporting electrolyte as employed in the cell. For aqueous electrochemistry a silver/silver chloride (3 M KCl) reference electrode was used. A carbon (d=3mm) working electrode was employed which was polished, prior to use, with 0.05µm alumina and rinsed with deionised water. The auxiliary electrode material was a platinum wire. A CH 660A potentiostat was employed for all electrochemical experiments. All solutions were degassed with pure argon for 15 min prior to electrochemical experiments. Differential pulse anodic stripping voltammograms (DPASV) were recorded with a 50 mV pulse height and a 0.2 s pulse period. For the preconcentration step the working electrode was immersed in a DMSO electrolyte solution of the complex under study for on average 600 seconds at the required deposition potential. The electrode was then removed and rinsed with MeCN and transferred to blank electrolyte solution for DPASV. All voltammetric experiments were carried out at room temperature, unless otherwise stated. For solid state voltammetric measurements a slurry of the complex was first prepared and then transferred onto the electrode surface. Before electrochemical studies the coatings were allowed to dry. After use, the electrode surface was renewed by rinsing with acetone, polishing with 0.05µm alumina and then sonicated in deionised water.

3. Results and discussion

3.1 Spectroscopic Characterisation

3.1.1 UV/Vis Spectroscopy

The UV/Vis spectrum for the α/β-$K_6P_2W_{18}O_{62}.15H_2O$ in DMSO exhibits maxima attributable to the tungstate framework with sharp rises into the UV with the spectrum agreeing with the literature [75]. The spectrum of $Os[bpy]_3{}^{2+}$ exhibits a series of absorptions [74]. The spectrum of a 0.05 mM DMSO solution of the complex exhibits all the absorbances detailed above with a λ_{max} of 307 nm and $\varepsilon = 31{,}740$ cm^{-1} M^{-1}.

3.1.2 IR Spectroscopy

The $[Os(bpy)_3]Cl_2$ salt exhibits the typical peaks in the range $1400 - 1650$ cm^{-1} which are characteristic of 2, 2' –bpy [62]. Two P-O stretches at 1090 and 1012 cm^{-1} occur for the α/β-$K_6P_2W_{18}O_{62}.15H_2O$ [75] The IR spectra of the complex exhibits the P-O stretches at 1089 and 1014 cm^{-1} for the heteropolyanion, and peaks in the range $1400 - 1650$ cm^{-1} for the 2, 2' –bpy moieties.

3.2 Electrochemical characterisation

3.2.1 Solution voltammetry of $[O(bpy)_3]_3[P_2W_{18}O_{62}]$

Before investigating the solution phase electrochemical studies of the complex it was important that we determine the electrochemical behaviour of the $Os(bpy)_3{}^{2+}$ moiety. A cyclic voltammogram of $Os(bpy)_3{}^{2+}$ gave the $Os^{3+/2+}$ metal-based redox processes with an $E_{1/2}$ = +0.677V and three one electron bipyridine ligand based reduction processes, with $E_{1/2}$ values of -1.495V ($bpy^{0/1-}$), -1.661V ($bpy^{1-/2-}$) and -1.970V ($bpy^{2-/3-}$) . The electrochemical behaviour of the Parent Dawson type heteropolyanion, α/β-$K_6P_2W_{18}O_{62}.15H_2O$ has previously been described [75].

In a 0.1M $TBAPF_6$ DMSO solution the complex exhibits a series of redox processes associated with the $Os^{3+/2+}$, bipyridine ligands along with two redox processes associated with the tungsten-oxo heteropolyanion framework. $E_{1/2}$ values of +0.521V ($Os^{3+/2+}$), -0.767V ($P_2W_{18}O_{62}{}^{6-/7-}$), -1.145V ($P_2W_{18}O_{62}{}^{7-/8-}$), -1.489V ($bpy^{0/1-}$), -1.657V ($bpy^{1-/2-}$) and -1.964 ($bpy^{2-/3-}$)

have been determined. It is important to stress that there was good agreement between these $E_{1/2}$ values for the complex and the $E_{1/2}$ values obtained for the individual cationic and anionic species in solution. Figure 1(a) illustrates the resulting cyclic voltammogram obtained for the complex when cycled through the $Os^{3+/2+}$ couple, at 10mV s^{-1} in 0.1M TBAPF$_6$ DMSO. The oxidised complex, namely $[Os(bpy)_3]^{3+}$, appears to be surface active as may be seen by the sharp nature of the corresponding reduction wave. In other words when the oxidised form of the complex is generated there is an interaction between it and the electrode surface. Upon oxidation there is a precipitation of a mixed anion salt namely, $[PF_6][Os(bpy)_3]_3[P_2W_{18}O_{62}]$, onto the carbon electrode surface, the main driving force behind this adsorption is the inherent insolubility of the complex in the solvent electrolyte system. This explanation has previously been employed by Hultgren *et al* [60] for their transition metal tris bypridine HPA complex.

The role of electrolyte was investigated and voltammetric studies on a DMSO solution of the complex containing 0.01M Bu$_4$NPF$_6$ were undertaken. Figure 1(b) shows that both the reduction and oxidation processes of the complex are now altered by the presence of $Os(bpy)_3^{2+}$ and also that there are differences that exist relative to the same processes in 0.1M Bu$_4$NPF$_6$. Figure 1(b) implies that in addition to the oxidised complex, the reduced complex now exhibits features that point to an interaction between it and the carbon surface due to the sharp nature of the bpy$^{0/1-}$ reduction step. To further investigate this a restrictive cyclic voltammogram was undertaken so as to encompass the two tungsten-oxo based processes, namely, $[P_2W_{18}O_{62}]^{6-/7-}$ and $[P_2W_{18}O_{62}]^{7-/8-}$. Figure 2(a) illustrates the resulting cyclic voltammogram when the electrode potential is swept between 0 and -1.35V. This figure shows that both the $[P_2W_{18}O_{62}]^{7-}$ and $[P_2W_{18}O_{62}]^{8-}$ species appear to indicate interaction with the electrode surface due to the sharp nature of their reoxidation waves. To further investigate the latter point, the potential of the working electrode was only swept to –0.90V, thereby only encompassing the $[P_2W_{18}O_{62}]^{6-/7-}$ redox system, this is seen in figure 2(b). Upon scan reversal the reoxidation wave loses its sharp nature and appears as a simple one electron diffusion wave. This suggests that the $[P_2W_{18}O_{62}]^{7-}$ species does not adsorb onto the electrode surface, and that it is only when $[Os(bpy)_3]_3[P_2W_{18}O_{62}]$ is reduced by two electrons that there appears

to be a precipitation onto the electrode surface of what is believed to be a mixed cation salt, $[Bu_4N]_2[Ru(bpy)_3]_3[P_2W_{18}O_{62}]$.

Differential pulse anodic stripping voltammetric (DPASV) experiments were performed so as to confirm the adsorption phenomenon observed in 0.01M electrolyte concentration. Figure 3 illustrates the DPASV of a modified carbon electrode in 0.1M Et_4NPF_6 after an accumulation step at -1.0V in 0.5mM $[Os(bpy)_3]_3[P_2W_{18}O_{62}]$ DMSO 0.01M Et_4NPF_6 solution for 600 secs. The potential of the working electrode is extended to 1.0V in order to prove that the $[Os(bpy)_3]^{2+}$ cation is part of the mixed cation salt which precipitates onto the electrode upon reduction of $[Os(bpy)_3]_3[P_2W_{18}O_{62}]$ during the accumulation step. Figure 3 shows stripping peaks for the $[P_2W_{18}O_{62}]^{8-/7-}$ and $[P_2W_{18}O_{62}]^{7-/6-}$ redox processes, at -0.822 and -0.475V, respectively. These are due to the oxidation of the $[Et_4N]_2[Os(bpy)_3]_3[P_2W_{18}O_{62}]$ and $[Et_4N][Os(bpy)_3]_3[P_2W_{18}O_{62}]$ mixed cation salts, respectively. Also present is the stripping peak associated with the $Os^{3+/2+}$ couple at +0.588V with an associated pre-peak at +0.434V, the latter being characteristic of a strongly adsorbed product on an electrode surface [77, 78]. These results clearly show that when the $[Os(bpy)_3]_3[P_2W_{18}O_{62}]$ is reduced to the $[P_2W_{18}O_{62}]^{8-}$ form, there is a precipitation onto the electrode surface of a mixed cation salt, $[Et_4N]_2[Os(bpy)_3]_3[P_2W_{18}O_{62}]$, with cations from the supporting electrolyte playing a role. To further prove that in 0.01M electrolyte the $[P_2W_{18}O_{62}]^{7-}$ form of the complex does not lead to precipitation onto the electrode surface the accumulation potential was held at the required potential so as to generate the $[P_2W_{18}O_{62}]^{7-}$ redox state. The electrode was then placed in fresh blank electrolyte and no stripping peaks were observed. This result proves that the $[P_2W_{18}O_{62}]^{7-}$ state of $[Os(bpy)_3]_3[P_2W_{18}O_{62}]$ is not surface active.

3.3   Thin Film voltammetry of $[Os(bpy)_3]_3[P_2W_{18}O_{62}]$

As discussed in the previous section the oxidative processes of the Os^{2+} centre exhibits characteristics pointing to an interaction between the complex and the electrode surface. As a result a film of the complex could be deposited onto the electrode surface by continuous redox switching through the osmium metal redox couple. Films were formed by cycling the potential of the glassy carbon electrode through the $Os^{3+/2+}$ redox process for 250 cycles from

a 0.1M TBAPF$_6$ DMSO solution of the starting complex. Figure 4 shows the resulting cyclic voltammogram obtained for the immobilised [Os(bpy)$_3$]$_3$[P$_2$W$_{18}$O$_{62}$] complex on a carbon electrode at pH 2.00. The cyclic voltammogram exhibits three clear bielectronic redox couples with E$_{1/2}$ values of -0.260, -0.446 and -0.687V, with the peak to peak separations all being less than 15mV. To calculate the number of electrons transferred in each redox step the full width at half-maximum (FWHM) for each couple is calculated. As is well known in the literature [77], the full width at half-maximum (FWHM) for a surface wave should be 90.6/n mV where n is the number of electrons involved, for the case of non-interacting neighbours within a film. From figure 4 FWHM values for the first, second and third redox waves are 86, 60 and 61mV respectively. This points to the last two redox processes being bielectronic in nature. However the FWHM values for these last two reductions for both films are higher than the 45.3mV value expected for a typical bielectronic process. Repulsive interactions within the film can be the cause for these higher than expected FWHM values [79, 80]. Despite the FWHM pointing to the first redox process being monoelectronic we believe it is bielectronic for two reasons. At slower scan rates a slight shoulder has been observed on the first redox process and it is well known that the first two monoelectronic processes are very close in potential. Secondly it is well know that the parent HPA can accept 6 electrons reversibly.

The P$_2$W$_{18}$O$_{62}$$^{6-}$ Dawson species is stable in pH's from 2.00 to 8.00 and its electrochemical behaviour depends upon the pH of the contacting electrolyte with some of the tungsten-oxo based redox processes involving protonation [75]. As a result we were interested in investigating the effect of solution pH on the redox activity of the film. With increasing pH, the three tungsten redox peaks move to more negative potentials with each couple showing a shift of 60-75 mV per pH unit, corresponding to approximately the addition of two protons, as observed with the solution phase species [75].

The stability of the film towards redox cycling was investigated at two pH values, namely 2.00 and 4.50. After cycling in pH 2.00 for 100 and 200 cycles, the percentage loss in global electroactivity associated with the [P$_2$W$_{18}$O$_{62}$]$^{6-/8-}$ redox process was 12.1 and 19.0%, respectively. The other two tungsten-oxo based redox processess showed similar percentage

losses. When the film is cycled in buffer pH 4.50 for 100 and 200 cycles, the percentage loss in global electroactivity associated with the $[P_2W_{18}O_{62}]^{6-/8-}$ redox process was 26.4 and 41.4%, respectively. The other two tungsten-oxo based redox processess showed similar percentage losses. The lower stability of the film towards redox cycling in pH 4.50 is linked to the pH dependent nature of the tungsten-oxo reductions, when at more alkaline pH's the availability of protons which accompany the reductions is less, relative to that in pH 2.00. Scan rate studies were also performed at both pH 2.00 and 4.50, it was found that the peak potentials were independent of scan rate and that the peak currents of the associated redox processes were directly proportional to scan rates of up to $2Vs^{-1}$ at both pH values.

3.4 Solid State Electrochemistry

When the redox composition of the complex microcrystals is switched between the Os^{2+} and Os^{3+} states, charge compensating counterions from the surrounding electrolyte must move into or out of the crystals in order to maintain electroneutrality within the film, a process known as "ion intercalation", according to equation 1 below:

$$[Os(bpy)_3]_3[P_2W_{18}O_{62}] + anion \rightarrow [Os(bpy)_3]_3[P_2W_{18}O_{62}][anion]_{(solid)} + e\text{-}.......(1)$$
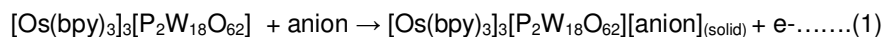
Figure 5(a) is the resulting cyclic voltammogram attained when a newly formed film of the complex is first exposed to redox cycling in aqueous 1M $LiClO_4$ electrolyte. What is apparent is the presence of the $Os^{3+/2+}$ redox couple with an associated $E_{1/2}$ of +0.544V and a peak to peak separation, ΔE_p, of 104mV. These values are in close agreement with those for the complex in 0.1 TBAP DMSO solution, in which the $E_{1/2}$ is +0.580V and ΔE_p is 96mV. Also it is clear from the figure 5(a) that there is no significant change in either the peak currents or potentials or the presence of what is termed "inert zones" during the initial "breaking-in" process, as seen with other systems [63]. A scan rate study was performed on the microcrystals and it was found that the peak currents for both the oxidation and reduction processes were dependent upon the square root of the scan rate.

The nature of the background electrolyte and its effect on the redox switching of the surface attached microcrystals of the complex was investigated. The $E_{1/2}$ positions along with the ΔE_p values in various electrolytes are two important parameters. A knowledge of these will give an indication on whether or not the material possesses rapid or slow anion insertion/expulsion and also if there is a difference in the insertion of a hydrophilic versus a hydrophobic anion into the crystals lattice [64]. Table 1 summarises the data obtained for the redox switching of the material through the $Os^{3+/2+}$ couple as a function of background electrolyte. It is clear that the ΔE_p values are all of similar value but there is a slight positive shift in the $E_{1/2}$ value from 0.775 to 0.803V when changing from the insertion into the crystal of a hydrophilic (NO_3^-) to a hydrophobic (PF_6^-) anion. This positive shift perhaps implies that the interior of the microcrystal is more hydrophilic in nature than hydrophobic.

Further information regarding the electrochemical behaviour of the solid material on the electrode surface can be attained by investigating the effect of the concentration of the supporting electrolyte on the voltammetric behaviour of the complex. This can yield information about presence of ionic interactions, differences in the stabilities between the oxidised and reduced forms of the material and the possible presence of ion partitioning. These studies have been undertaken with a variety of solid state redox active materials [65-68]. The parameter of interest is the $E_{1/2}$ value of the $Os^{3+/2+}$ redox couple. Previously authors have described two limiting cases when discussing the effect of electrolyte concentration upon the $E_{1/2}$ value for a redox couple of a surface confined solid state material, namely the "thin film" and "thick film" models. The former is where the $E_{1/2}$ is independent of the electrolyte concentration whilst the latter is when a Nernstian shift of 59mV per change in electrolyte concentration for monoelectronic processes is obtained. However some systems have exhibited what is termed *"sub-Nernstian"* behaviour, where a potential analogous to the *"Donnan potential"* [69, 81] is established due to the presence of a charged layer at the solid/electrolyte barrier arising from the effect of ion partitioning. To investigate which model would fit the behaviour of our microcrystals the effect of electrolyte concentration on the $E_{1/2}$ was investigated. Table 1 summarises the results obtained for the Nernst plots in several aqueous electrolytes with figure 5(b) illustrating an obtained plot. They all show *"sub-*

Nernstian" behaviour thereby pointing to the presence of a charged layer at the solid / electrolyte barrier.

It is also of interest whether or not the redox processes associated with the tungsten-oxo cage could be electrochemically accessed for the immobilised microcrystals of our complex. Figure 6(a) illustrates the repetitive cyclic voltammograms for solid deposits of $[Os(bpy)_3]_3[P_2W_{18}O_{62}]$ in 1.0M $HClO_4$ electrolyte. What is observed is the gradual growth in the current associated with the first two tungsten-oxo based processes upon continual scanning. There is no apparent shift in the $E_{1/2}$ values during cycling but there is a dramatic growth in the currents associated with these tungsten-oxo processes, this possibly being linked to structural change within the microcrystals.

SEM images of the immobilised microcrystals of $[Os(bpy)_3]_3[P_2W_{18}O_{62}]$ were taken before and after voltammetric cycling in 1.0 M $HClO_4$. Figure 6(b) shows an image of the layer after being vacuum dried but prior to voltammetric cycling. The immobilised Os layer appears to exist as an array of particles, ranging in sizes from approximately 100 μm to sub-μm. Figure 6(c) illustrates the SEM image obtained after the film was cycled in 1.0 M $HClO_4$ for approximately 50 scans. From these SEM images it appears that when the deposit is cycled in the 1.0M $HClO_4$ the macroscopic structure of the material changes, with possible fusing together of the deposits. However, at this stage it is difficult to conclude the precise change occurring and future work shall be undertaken in this regard. In addition, so as to ascertain the elemental composition of the microcrystals a preliminary EDX spectra of solid $[Os(bpy)_3]_3[P_2W_{18}O_{62}]$ immobilised on a glassy carbon electrode was undertaken. Responses were clearly present for osmium and carbon, from the $[Os(bpy)_3]^{2+}$ moiety, and phosphorous, tungsten and oxygen from the $[P_2W_{18}O_{62}]^{6-}$ HPA moiety. Hydrogen is undetectable using EDX due to its low atomic number.

4.0   Conclusion

$[Os(bpy)_3]_3[P_2W_{18}O_{62}]$ has been synthesised and fully characterised. Solution phase electrochemical behaviour of the complexes showed that the $[Os(bpy)_3]^{3+/2+}$ redox process changed from solution phase to a surface based process due to the presence of the larger anion $[P_2W_{18}O_{62}]^{6-}$. The concentration of the supporting electrolyte was seen to have a marked effect on the $[P_2W_{18}O_{62}]^{7-/8-}$ redox process. Upon lowering of the electrolyte concentration to 0.01M, the $[P_2W_{18}O_{62}]^{8-}$ form of the complex was seen to adsorb onto the electrode surface leading to the formation of a mixed cation salt. The complex was found to adsorb onto electrode surfaces when redox switched between the transition metal complex. Voltammetric studies of the adsorbed film exhibited the same pH dependence for the tungsten-oxo framework of the HPA as in solution. The films were also found to exhibit better stability towards redox cycling in pH 2.00 as compared to pH 7.00 solution. Mechanically attached solid state films of $[Os(bpy)_3]_3[P_2W_{18}O_{62}]$ have been formed on carbon electrodes. The redox switching of the films through the transition metal process was seen to be reversible. The effect of both the nature and concentration of the supporting aqueous electrolyte was investigated with the Nernst plots showing sub-Nernstian behaviour.

Acknowledgements

References

[1]   C. Cibert, C. Jasmin, Biochem. Biophys. Res. Commun., 108 (1982) 1424.

[2]   M. Raynaud, J.C. Chermann, F. Plata, C. Jasmin, G. C. Mathe, R. Acad., Ser. D. 272 (1971) 347.

[3]   W. Rosenbaum, D. Dormont, B. Spire, E. Vilmer, M. Gentilini, C. Griscelli, L. Montagnier, F. Barre-Sinoussi, J.C. Chermann, Lancet (1985) 450.

[4]   T.Yamase, Mol. Eng., 3 (1993) 241.

[5]   X.H. Wang, J.F. Liu, Y.G Chen, Q. Liu, J.T. Liu, M.T. Pope, J.Chem.Soc.,Dalton Trans., 7 (2000) 1139.

[6]   J.C. Bart, F.C. Anson, J.Electroanal.Chem., 390 (1995) 11.

[7]   C. Rong, F.C. Anson, Inorg.Chem., 33 (1994) 1064.

[8]   M. Sadakane, E. Steckhan, J.Mol.Catal.A. Chemical 114 (1996) 221.

[9]   M.T. Pope, A. Muller, Agnew. Chem. Int. Ed. Engl., 30 (1991) 34.

[10]   E. Steckhan, C. Kandzia, Synlett., (1992) 139.

[11]   C.L. Hill, R.B. Brown, J.Am.Chem.Soc., 108 (1986) 536.

[12]   A.A. Shatalov, D.V. Evtuguin, C.P. Neto, Carbohydrate polymers, 43 (2000) 23.

[13]   L. Yang, H. Naruke, T. Yamase, Inorg. Chem. Comm., 6 (2003) 1020.

[14]   J.Y. Niu, Z.L. Wang, J.P. Wang, Polyhedron 23 (2004) 773.

[15]   L. Lisnard, A. Dolbecq, P. Mialane, J. Marrot, F. Secheresse, Inorg. Chim. Acta., 357 (2004) 845.

[16]   S. Dong, X. Xi, M. Tian, J. Electroanal. Chem., 385 (1995) 227.

[17]   B. Keita, A. Belhouari, L. Nadjo, R. Contant, J. Electroanal. Chem., 381 (1995) 243.

[18]   X. Xi, S. J. Dong, Mol. Catal. A: Chemical 114 (1996) 257.

[19]   T. McCormac, B. Bidan, G. Fabre, J. Electroanal. Chem., 427 (1997) 155.

[20]   J.E. Toth, F.C. Anson, J. Am. Chem. Soc.. 111 (1989) 2444.

[21]   W. Sun, H. Liu, J. Kong, G. Xie, J. Dong, J. Electroanal. Chem., 437 (1997) 67.

[22]   W. Sun, F. Yang, H. Liu, J. Kong, S. Jin, G. Xie, J. Dong, J. Electroanal. Chem., 451(1998) 49.

[23]   B .Keita, F. Girard, L. Nadjo, R. Contant, M. Abbessi, J.Electroanal.Chem., 508 (2001) 70.

[24]   B. Keita, E. Abdeljalil, L. Nadjo, R. Contant, R. Belgiche, Electrochem.Commun., 3 (2001) 56.

[25]   S. Dong, M. Liu, J. Electroanal. Chem., 372 (1994) 95.

[26]   J.E. Toth, J.D. Melton, D. Cabelli, B.H.J. Bielski, F.C. Anson, Inorg.Chem., 29 (1990) 1952.

[27]   J.C. Bart, F.C. Anson, J.Electroanal.Chem., 390 (1995) 11.

[28]   N.I. Kuznetsova, L.I. Kuznetsova, V.A. Likholobov, J.Mol.Cat.A., 108 (1996) 135.

[29]   K. Essaadi, B. Keita, L. Nadjo, J.Electroanal.Chem., 367 (1994) 275.

[30]   B. Keita, K. Essaadi, L. Nadjo, M. Desmadril, Chem.Phys.Lett., 237 (1995) 411.

[31]   B. Keita, K. Essaadi, L. Nadjo, R. Contant, Y. Justum, J. Electroanal. Chem., 404 (1996) 271.

[32]   B. Keita, Y.W. Lu, L. Nadjo, R. Contant, M. Abbessi, J. Canny, M. Richet, J. Electroanal. Chem., 477 (1999) 146.

[33]   B. Keita, L. Nadjo, J.Electroanal.Chem., 191 (1985) 441.

[34]   B. Keita, L. Nadjo, J.Electroanal.Chem., 227 (1987) 77.

[35]   B. Keita, L. Nadjo, J.P. Haeussler, *J.Electroanal.Chem.*, 243 (1988) 481.

[36]   K. Unoura, A. Iwashita, E. Itabashi, N. Tanaka, Bull.Chem.Soc.Jpn., 57 (1984) 597.

[37]   B. Keita, L. Nadjo, J.Electroanal.Chem., 191 (1985) 441.

[38]   B. Keita, L. Nadjo, J.Electroanal.Chem., 354 (1993) 295.

[39]   B. Watson, M.A. Barteau, L. Haggerty, A.M. Lenholf, R.S. Weber, Langmuir. 8 (1992) 1145.

 [40]   Z.Y. Tang, S.Q. Liu, E.K. Wang, S.J. Dong, E.B. Wang, Langmuir. 16 (2000) 5806.

[41]   P. Wang, X.P Wang, G.Y. Zhu, Electroanalysis. 12 (2000) 1493.

[42]   B. Keita, E.A. Abdeljalil, F. Girard, S. Gerschwiler, L. Nadjo, R. Contant, C. Haut, J.Solid.State.Electrochem., 3 (1999) 446.

[43]   B. Keita, E.A. Abdeljalil, L. Nadjo, R. Contant, R. Belgiche, *Electrochem.Com.3*. 3 (2001) 56.

[44]   X. Xi, S. Dong, J.Mol.Catal.A. Chemical., 114 (1996) 257.

[45]   S. Dong, M. Liu, Electrochim.Acta., 39 (1994) 947.

[46]   B. Fabre, G. Bidan, M. Lapkowski, J.Chem.Soc., Chem.Commun., (1994) 1509.

[47]   A. Mahmoud, B. Keita, L. Nadjo, O. Oung, R. Contant, S. Brown, Y. de Kouchkovsky, J.Electroanal.Chem., 463 (1999) 125.

[48]   H.Y. Sung, H.S. So, W.K. Paik, Electrochim.Acta., 39 (1994) 645.

[49]   B. Keita, L. Nadjo, J.Electroanal.Chem., 247 (1988) 157.

[50]   B. Wang, S. Dong, Electrochim.Acta., 41 (1996) 895.

[51]   X. Xi, S. Dong, Electrochim.Acta., 40 (1995) 2785.

[52]   B. Wang, S. Dong, J.Electroanal.Chem., 328 (1992) 245.

[53]   X. Xi, S. Dong, J.Mol.Catal.A. Chemical. 114 (1996) 257.

[54]   C. Rong, F.C. Anson, Inorg.Chim.Acta., 242 (1996) 11.

[55]   L.Cheng, J.A. Cox, Electrochem.Comm., *3* (2001) 285.

[56]   D. Ingersoll, P.J. Kulesza, L.R. Faulkner, J.Electrochem.Soc., 141 *(*1994) 140.

[57]   A. Kuhn, F.C. Anson, Langmuir 12 (1996) 5481.

[58]   G.M. Kloster, F.C. Anson Electrochimica. Acta., 44 (1999) 2271.

[59]   L. Cheng, J. Liu, S. Dong Anal. Chim. Acta., 417 (2000) 133.

[60]   V.M. Hultgren, A.M. Bond, A.G. Weld, J. Chem. Soc. Dalton. Trans., (2001) 1076.

[61]   X.L. Wang, Z.B. Han, E.B. Wang, H. Zhang, C.W. Hu, Electroanalysis 15, 8 (2003) 1460.

[62]   Z. Han, E. Wang, G. Luan, Y. Li, C. Hu, P. Wang, N. Hu, H. Jia, Inorg. Chem. Commun., 4 (2001) 427.

[63]   A.M. Bond, S. Fletcher, P.G. Symons, Analyst 123 (1998) 1891.

[64]   F. Marken, R.G. Compton, C.H. Goeting, J.S. Foord, S.D. Bull, S.G. Davies Electroanalysis 1 (1998) 821.

[65]   F.A. Armstrong, H.A. Heering, J. Hirst J Chem. Soc. Rev., 26 (1997) 169.

[66]   J. Redepenning, H.M. Tunison, J. Moy J. Phys. Chem., 98 (1994) 2426.

[67]   A.M. Bond, F. Marken, C.T Williams, D.A. Beattie, T.E Keyes., R.J. Forster, J.G. Vos J Phys. Chem. B., 104 (2000) 1977.

[68]   J. Redepenning, B. R. Miller, S. Burnham. Anal. Chem., 66 (1994) 1560.

[69]   R. J. Forster, T. E. Keyes, A. M. Bond. J. Phys. Chem. B. 104 (2000) 6389.

[70]   C. Yang, G. He, R. Wang, Y. Li, J. Electroanal. Chem., 471 (1999) 32.

[71]   M. S. Wrighton, Science 231 (1986) 32.

[72]   A. Tredicucci, C. Gmachi, F. Capasso, D. L. Sivco, A. L. Hutchinson, Y. A. Cho, Nature, 396 (1998) 350.

[73]   D.K. Lyon, W.K. Miller, T. Novet, P.J. Domaille, E. Evitt, D.C. Johnson, R.G. Finke, J. Am. Chem. Soc., 113 (1991) 7209.

[74]   C. Creutz, M. Chou, T.L. Netzel, M. Okumura, N. Sutin, J.Am.Chem.Soc., (1980) 1309.

[75]   T. McCormac, G. Bidan, B. Fabre J.Electroanal.Chem., 425 (1997) 49.

[76]   Creutz. J. Am. Chem. Soc. (1980) 1309.

[77]   A.J Bard, L.R Faulkner Electrochemical Methods Wiley & Sons Inc New York (2001).

[78]   R.H Wopshall, I. Shain, Anal. Chem., 39 (1967) 1514.

[79]   E Laviron, J. Electroanal. Chem., 105 (1979) 35.

[80]   D.F Smith, K Willman, K Kuo, R.W Murray, J. Electroanal. Chem., 95 (1979) 217.

[81]   N. Fay, A. Kennedy, E. Dempsey, T. McCormac, J. Electroanal. Chem., 95 (2003) 217.

Table 1: Electrochemical parameters ($E_{p,a}$, $E_{p,c}$, $E_{1/2}$, ΔE_p) and slopes of the half wave potentials vs. log [anion] plots, for the redox switching of microcrystals of $[Os(bpy)_3]_3[P_2W_{18}O_{62}]$ in various aqueous electrolytes. Carbon Working electrode (Area = $0.0707 cm^2$). Scan rate = 100 mVs^{-1}.

Electrolyte	$E_{p,a}$ (Volts vs. Ag/AgCl)	$E_{p,c}$ (Volts vs. Ag/AgCl)	ΔE_p (mV)	$E_{1/2}$* (Volts vs. Ag/AgCl)	Slope $E_{1/2}$ vs log [X⁻] (mV)
NH_4PF_6	0.856	0.749	107	0.803	40.5
$LiClO_4$	0.818	0.722	96	0.770	29.3
KNO_3	0.824	0.725	99	0.775	19.5

* 1.0M electrolyte concentration

17

Figure Legends

Figure 1(a)   Cyclic voltammogram of a 0.5mM solution of $[Os(bpy)_3]_3[P_2W_{18}O_{62}]$ in DMSO 0.1M tetrabutylammonium hexafluorophosphate at a glassy carbon electrode ($A = 0.0707$ cm^2). Scan rate = 10 mV s^{-1}.

Figure 1(b)   Cyclic voltammogram of a 0.5mM solution of $[Os(bpy)_3]_3[P_2W_{18}O_{62}]$ in DMSO 0.01M tetrabutylammonium hexafluorophosphate at a glassy carbon electrode ($A = 0.0707$ cm^2). Scan rate = 10 mVs^{-1}.

Figure 2(a)   Cyclic voltammogram of a 0.5mM solution of $[Os(bpy)_3]_3[P_2W_{18}O_{62}]$ in DMSO 0.01M tetrabutylammonium hexafluorophosphate at a glassy carbon electrode ($A = 0.0707$ cm^2) between 0.00 and -1.35V. Scan rate = 10 mVs^{-1}.

Figure 2(b)   Cyclic voltammogram of a 0.5mM solution of $[Os(bpy)_3]_3[P_2W_{18}O_{62}]$ in DMSO 0.01M tetrabutylammonium hexafluorophosphate at a glassy carbon electrode ($A = 0.0707$ cm^2) between 0.00 and -1.00V. Scan rate = 10 mVs^{-1}.

Figure 3   Differential anodic stripping voltammogram of a modified glassy carbon ($A = 0.0707$ cm^2) electrode in 0.1M Et$_4$NPF$_6$ MeCN, after accummulation in 0.5mM of $[Os(bpy)_3]_3[P_2W_{18}O_{62}]$ in DMSO 0.01M Et$_4$NPF$_6$ at -1.25V for 600s.

Figure 4   Cyclic voltammogram of a thin film of $[Os(bpy)_3]_3[P_2W_{18}O_{62}]$ immobilised on a carbon working electrode ($A = 0.0707$ cm^2) cycled in pH 2.00 buffer. Scan rate = 100 mV s^{-1}.

Figure 5(a)   Cyclic voltammograms of an $[Os(bpy)_3]_3[P_2W_{18}O_{62}]$ solid deposit immobilised onto a carbon electrode ($A = 0.0707$ cm^2) in 1.0 M LiClO$_4$. Scan rate = 100 mV s^{-1}

Figure 5(b)   Plot of peak potentials E_{anod} (♦), $E_{1/2}$ (■) and E_{cath} (▲) versus the logarithm of the concentration of NH_4PF_6.

Figure 6(a)   Repetitive cyclic voltammograms for $[Os(bpy)_3]_3[P_2W_{18}O_{62}]$ solid deposits immobilised on a glassy carbon electrode ($A = 0.0707cm^2$) in aqueous 1.0M $HClO_4$ with the 1st (inner), 20th (middle) and 50th (outer) cycles being shown. Scan rate = 10 mVs^{-1}.

Figure 6(b)   SEM image of a solid deposit of $[Os(bpy)_3]_3[P_2W_{18}O_{62}]$ prior to redox cycling

Figure 6(c)   SEM image of a solid deposit of $[Os(bpy)_3]_3[P_2W_{18}O_{62}]$ after cycling in 1M $HClO_4$

Figure 1(a)
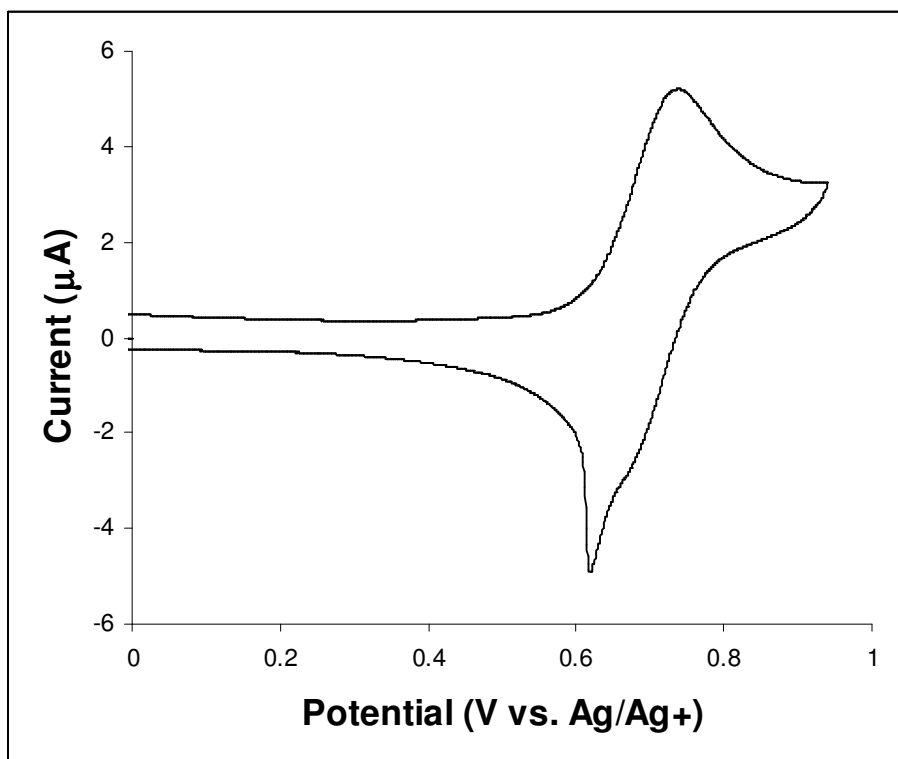
Figure 1(b)
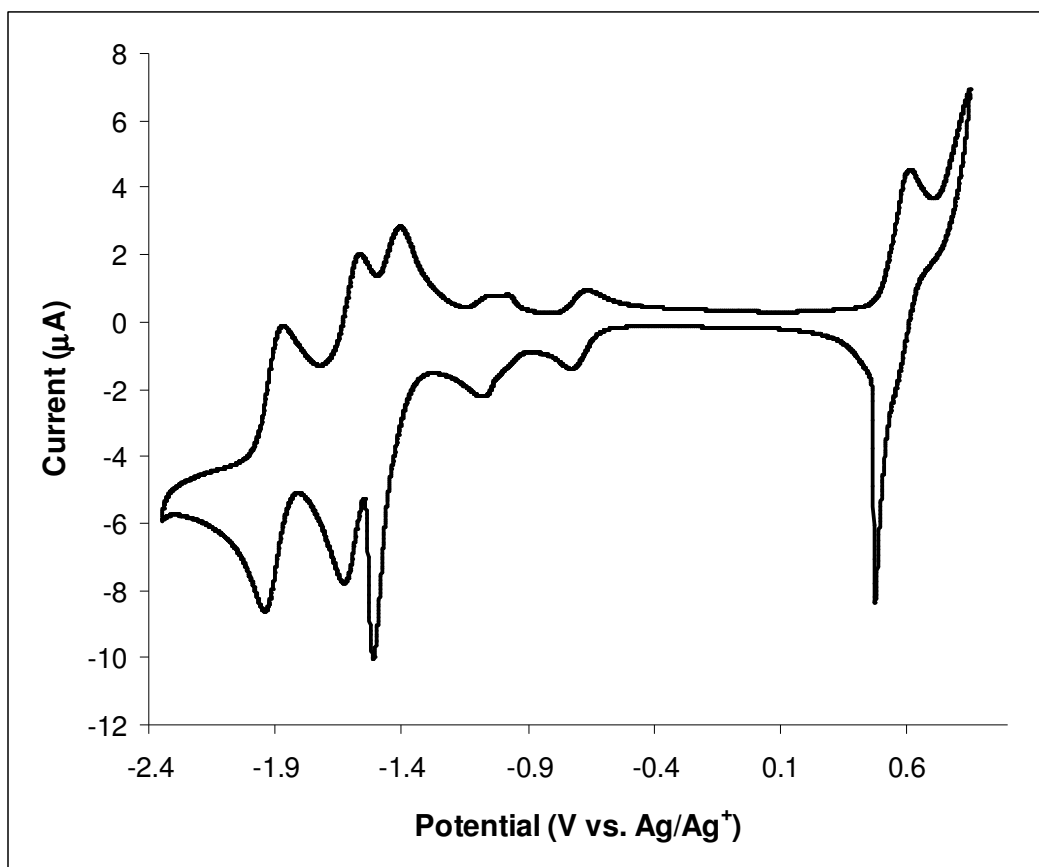
Figure 2(a)
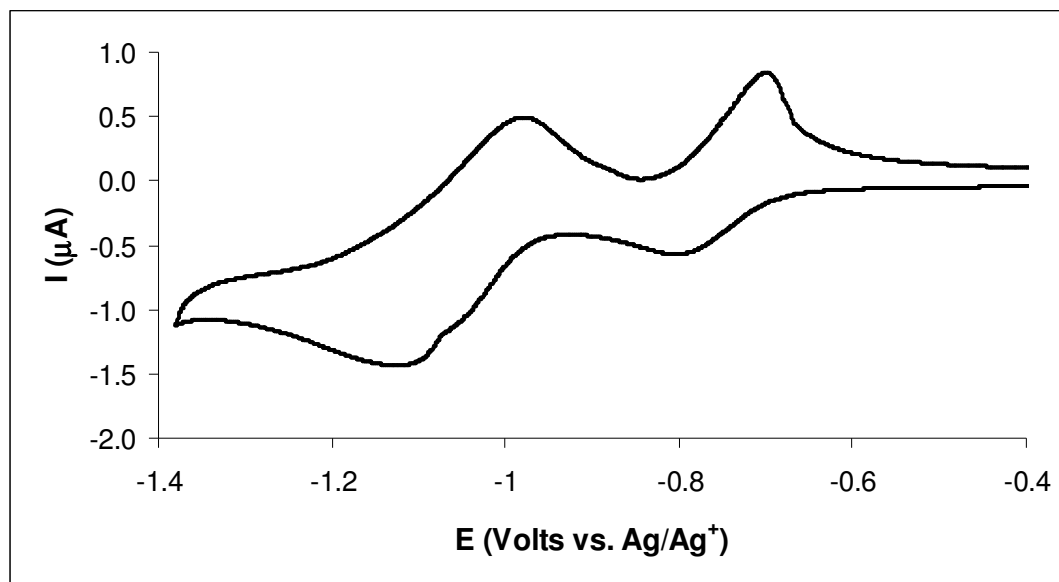
Figure 2(b)
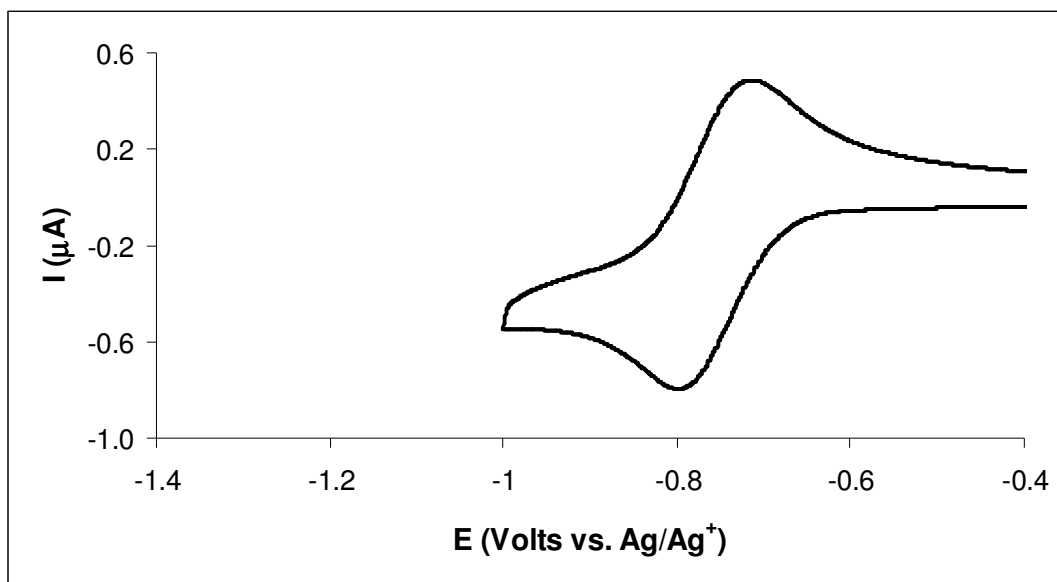
Figure 3
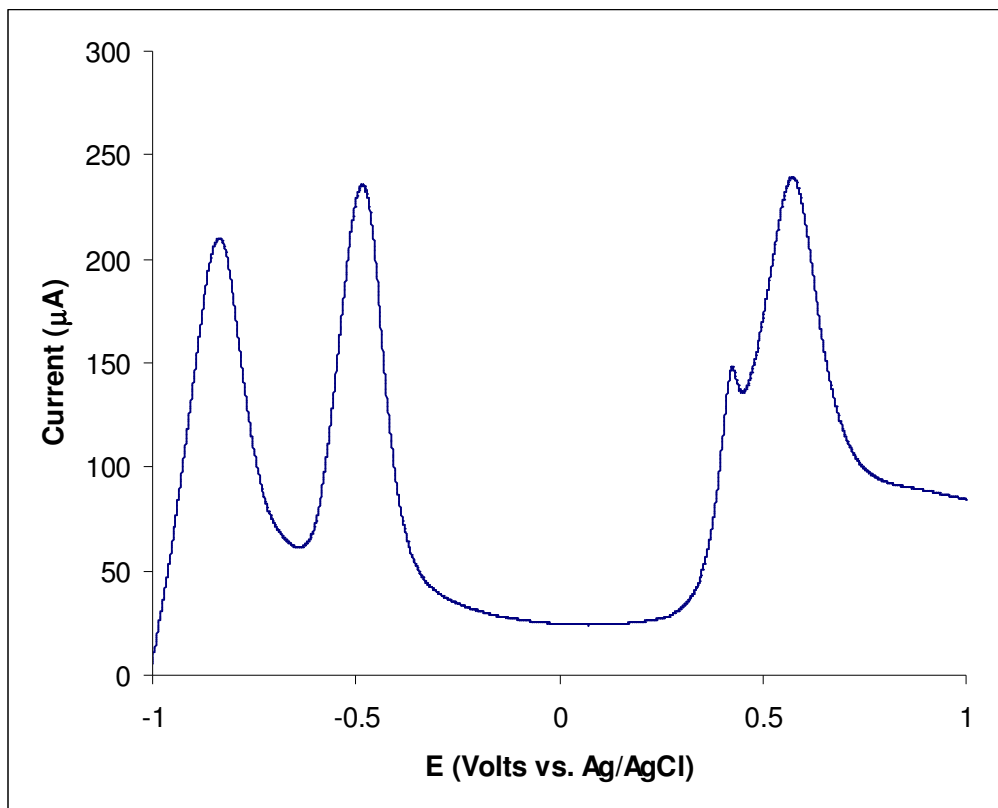
Figure 4
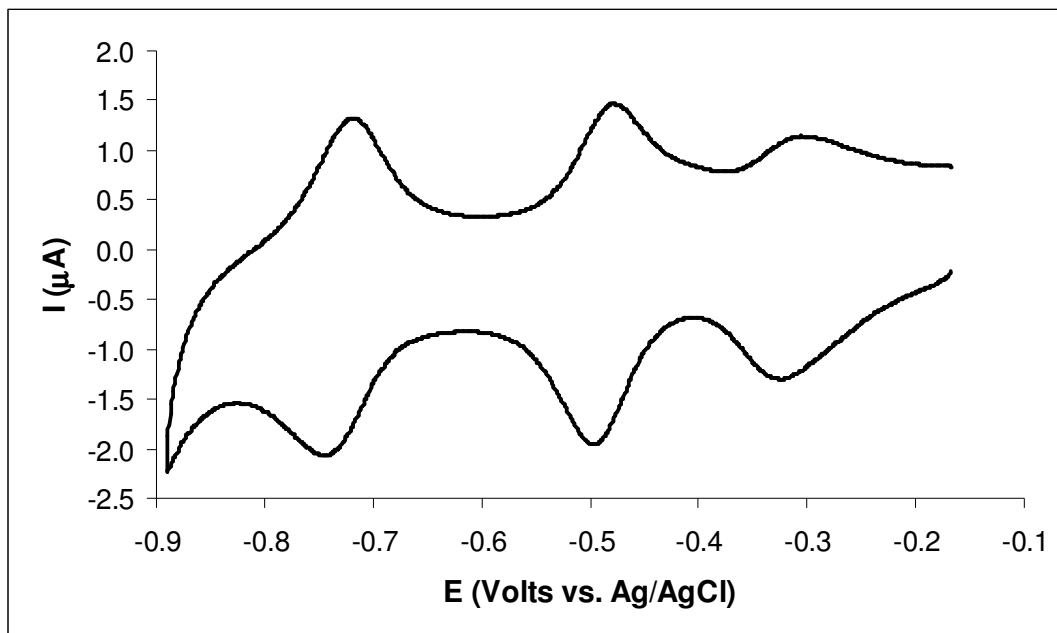
Figure 5(a)
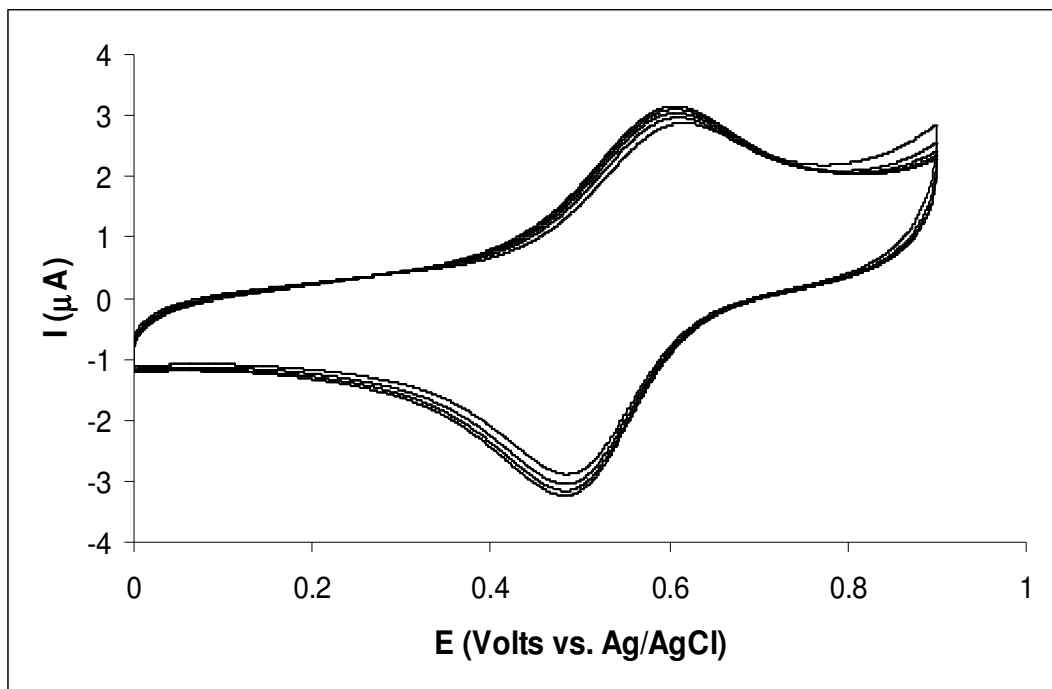
Figure 5(b)
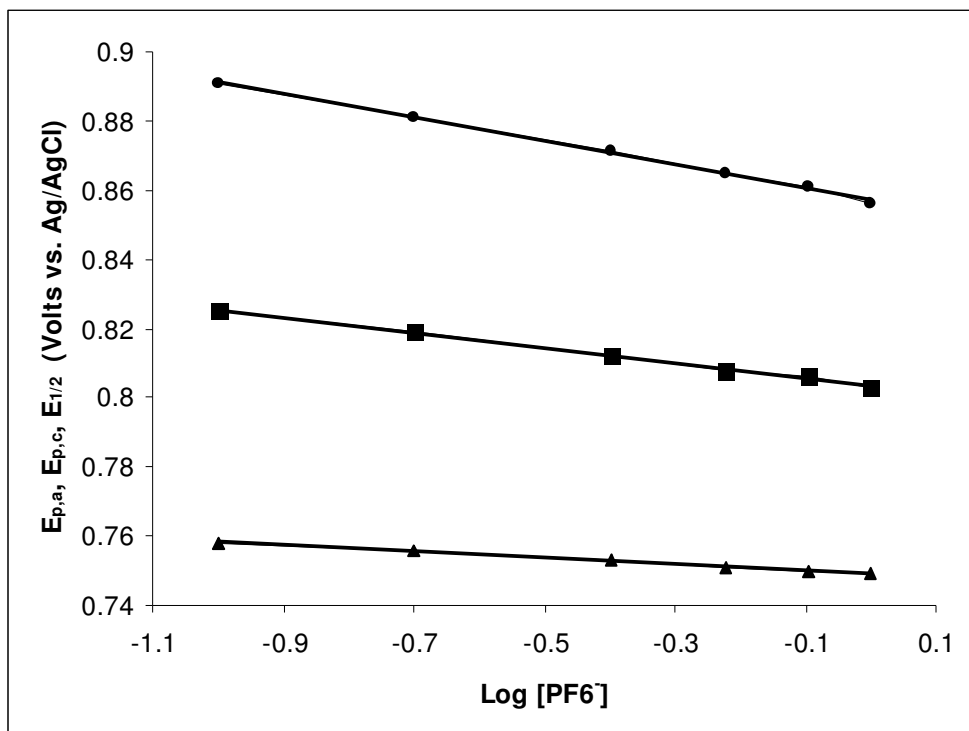
Figure 6(a)

Figure 6(b)

Figure 6(c)